Properties of an N=4 optimized quasi-isodynamic configuration

W.A. Cooper[3], M.I. Mikhailov[1], C. Nührenberg[2] J. Nührenberg[2] and V.D. Shafranov[1]

[1] *Russian Reserch Center "Kurchatov Institute", Moscow, Russia*

[2] *IPP, EURATOM Association, Germany*

[3] *CRPP, EURATOM Association, EPFL, Switzerland*

Introduction

It was shown earlier by computational optimization and partly by analytical consideration [1] that in quasi-isodynamic [2] configurations with poloidally closed contours of B the requirements of small neoclassical transport, small bootstrap current, good collisionless fast-particle confinement and high plasma-pressure stability limit can be reconciled. For the reference N = 6 configuration [1], the plasma-pressure global-stability limit is $\langle\beta\rangle \approx 0.1$. It was shown also that with increasing number of periods the stability limit grows (see. e.g. [3]). Here the possibilities of the quasi-isodynamic configurations with poloidally closed contours of B and smaller number of periods are investigated. Results of the integrated optimization of an N = 4 stellarator with aspect ratio A = 8 and $\langle\beta\rangle \approx 0.05$ are presented. Such properties as neoclassical transport in the $1/\nu$ regime (effective ripple), bootstrap current (normalized structural factor), collisionless fast-particle confinement (closure of the second-adiabatic-invariant contours), resistive-interchange, Mercier and ballooning modes stability are taken into account during the computational optimization. The global-mode stability is investigated with the CAS3D code subsequently to obtain growth rates of nonlocal modes.

Neoclassical properties

In Fig. 1 it is seen that the qualitative structure of the magnetic field strength described in [1] can be realized in a confinement domain with aspect ratio 8 and 4 periods, too: poloidally closed contours of B, concave surfaces of constant B as seen by reflected particles and an absolute minimum of B, which here is obtained with $\langle\beta\rangle \approx 0.05$. A special feature is the shape of the surfaces of constant B shown near $B_{\max}$: they are hyperboloid-like so that passing particles near the plasma center, which may be subject to collisionless stochastic diffusion due to a thin island in the topography of B on a magnetic surface, will transform into reflected particles at larger radius and so be confined as is seen from the contours of the second adiabatic invariant shown in Fig. 2 which indicate collisionless confinement up $s \approx 0.4$. Actual computation of collisionless orbits of α-particles, see Fig. 3 left, indeed shows very good confinement up to $\frac{2}{3}$ of the plasma radius.

Elimination of the bootstrap current in the long-meam-free-path regime and smallness of the neoclassical $1/\nu$ regime were part of the optimization goal, too. In Fig. 3, right, the result achieved for the bootstrap current density is compared to the one of W7-X [5], in which this current density is already strongly reduced. This result is in line with the approximate localization of the parallel current density to each period [1], see Fig. 4, left. Finally, Fig. 4, right, shows the equivalent neoclassical ripple which is small, too.

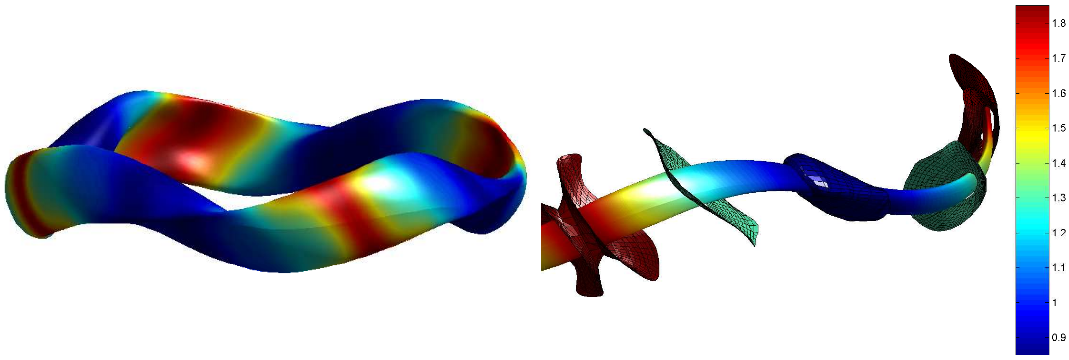

Figure 1: Left: Boundary magnetic surface showing the magnetic topography. Right: Inner magnetic surface and surfaces of B showing the magnetic topography.

MHD properties

The mhd stability of the configuration found is characterized as follows. The free-boundary stability is investigated at $\langle\beta\rangle \approx 0.05$ and 0.075. With a fourier-mode window comprising 30 poloidal and 33 toroidal mode indices, see Fig. 5 (left), instability is shown at $\langle\beta\rangle \approx 0.075$ with a growth time of $\approx 3\tau_{\mathrm{A}}$ (with the notation of [1]), while stability prevails at 0.05 and the marginal point is approximately $\langle\beta\rangle \approx 0.06$. So, the configuration is stable at $\langle\beta\rangle \approx 0.05$ against large-scale modes. The instability against fine-scale modes at this value of $\langle\beta\rangle$ is investigated with a fourier-mode window extending to $m_{\mathrm{poloidal}} = 36$ and $n_{\mathrm{toroidal}} = 25$; this mode is marginally unstable as is seen in Fig. 5 (right); it exhibits the typical ballooning signature as is seen in Fig. 6.

Summary

A case study of a quasi-isodynamic configuration with poloidally closed contours of B has been described. The resulting geometry of the configuration is shown in Fig. 7.

Acknowledgments

Part of the computations of this work has been performed on the NIFS LHD Numerical Analysis Computer SX-8. This work was supported in part by the Russian Foundation for Basic Research, project no 09-02-0142-a and by grant 2457.2008.2 of President of Russian Federation for state support of leading scientific school.

References

[1] A.A. Subbotin et al, Nucl. Fusion **46** (2006) 921.

[2] S.Gori, W. Lotz, J. Nührenberg, in Proc. Joint Varenna-Lausanne Int. Workshop on Theory of Fusion Plasmas 1996 (Bologna: Editrice Compositori, 1997) p.335.

[3] M.I. Mikhailov et al, in Theory of Fusion Plasmas: Joint Varenna-Lausanne International Workshop, edited by J. W. Connor, O. Sauter, and E. Sindoni, AIP 871, 388 (2006).

[4] A. Weller et al, *PPCF* **45**, A285 (2003).

[5] Yu. Turkin et al, Fusion Sci. Technol. **50** (2006) 387.

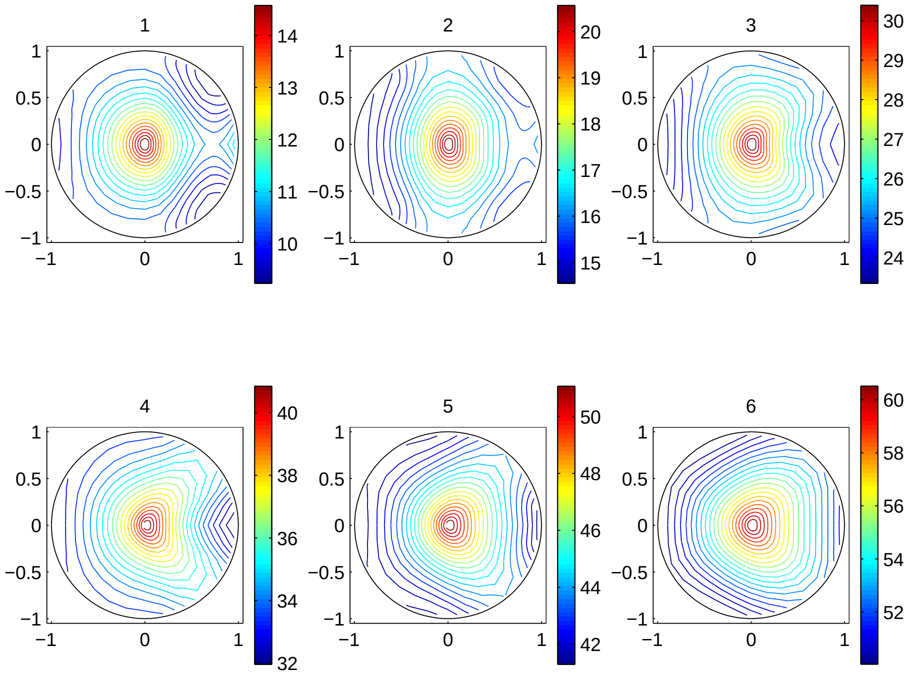

Figure 2: Structure of $\mathcal{J}$ in the configuration obtained for different values of B, B_{ref}, at which trapped particles are reflected; 1 - near the minimum of B, 6 - near the maximum of B.

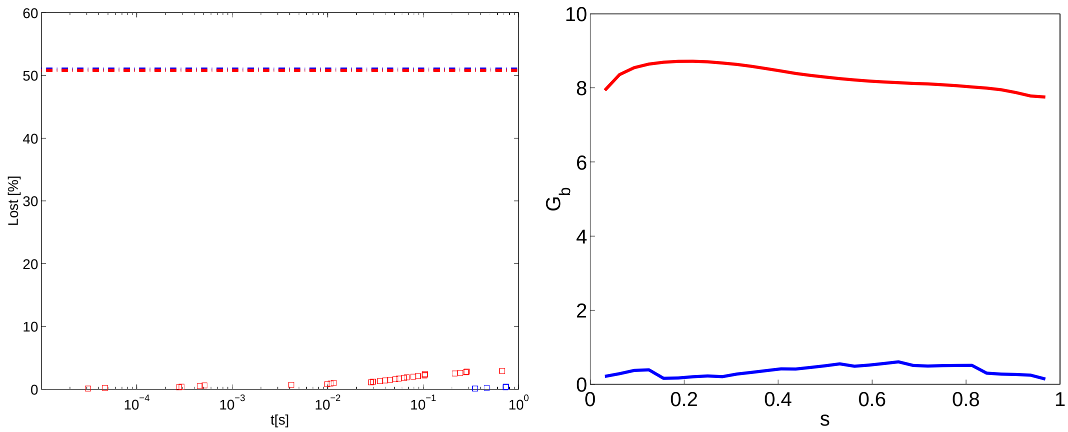

Figure 3: Left: Cumulative collisionless α-particle losses for particles started at $\frac{1}{2}$ and $\frac{2}{3}$ of the plasma radius. Right: Comparison of normalized bootstrap current density for W7-X (red) and the configuration described here.

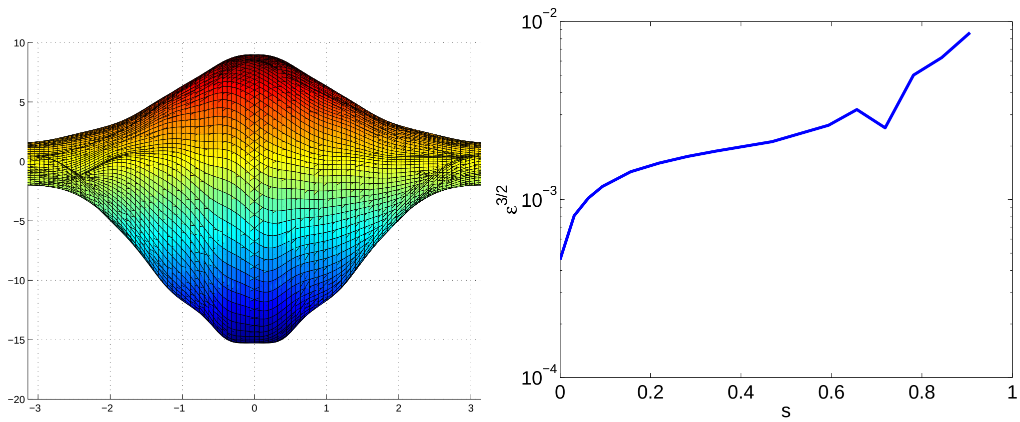

Figure 4: Left: Poloidal view of the topography of $\vec{j}\cdot\vec{B}/B^2$ at half the plasma radius as a function of poloidal and toroidal magnetic coordinate. Right: Equivalent neoclassical ripple (in the form $\varepsilon^{\frac{3}{2}}$) as a function of normalized toroidal flux.

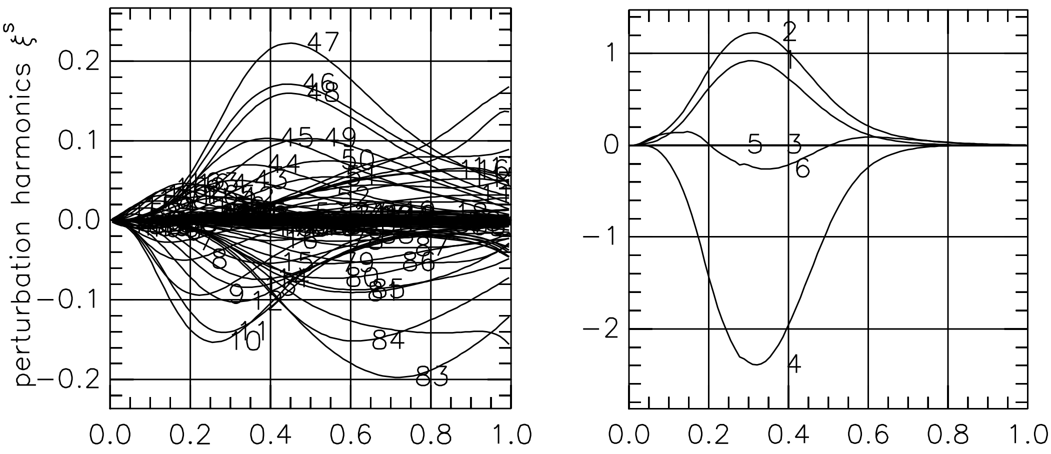

Figure 5: Left: Structure of an unstable free-boundary mode in the $\langle\beta\rangle \approx 0.075$ equilibrium computed for the $\langle\beta\rangle \approx 0.05$ configuration found. Shown are the Fourier component in magnetic coordinates of $\vec{\xi} \cdot \nabla s$. Right: Contributions from terms (1 - 5) of mhd-stability functional for a fine-scale internal mode; their sum, label 6, shows the mode to be marginally unstable.

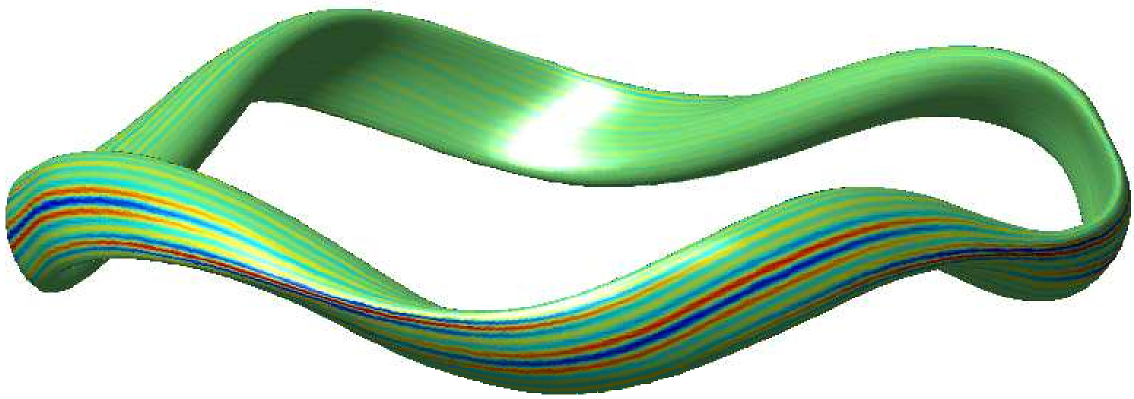

Figure 6: Structure of a weakly unstable ballooning mode in the $\langle\beta\rangle \approx 0.05$ equilibrium found. Shown is $\vec{\xi} \cdot \nabla s$ in magnetic coordinates at the flux surface of maximum amplitude.

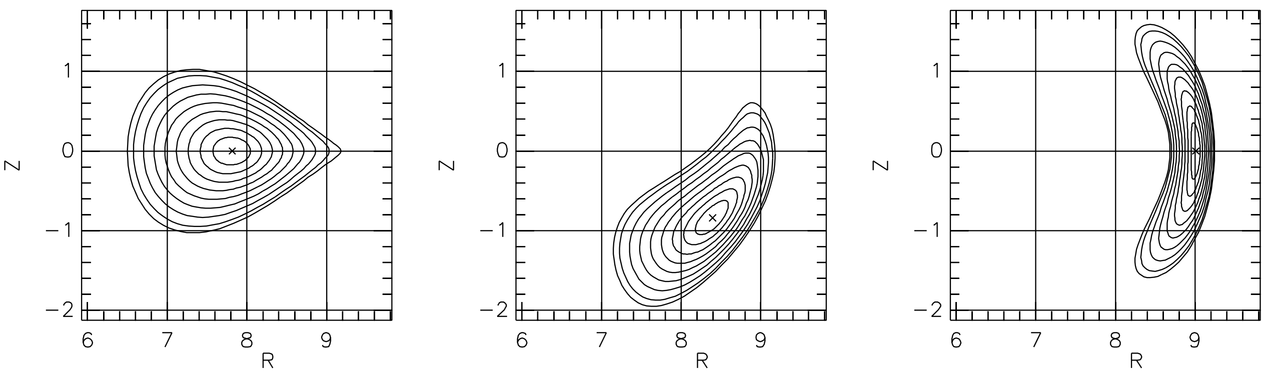

Figure 7: Cross sections of magnetic surfaces of the configuration found along half a period beginning with the minimum of B and ending at the maximum of B.